

Effect of Medium Properties on Convergence Rates of Multigrid Solutions of Laminar Flows in Permeable Structures

Maximilian S. Mesquita and Marcelo J.S. de Lemos*

*Departamento de Energia – IEME
Instituto Tecnológico de Aeronáutica – ITA
12228-900 - São José dos Campos - SP – Brazil*
* Corresponding author. E-mail: delemos@ita.br

Abstract

The present work investigates the efficiency of the multigrid method when applied to solve laminar flow in a two-dimensional tank filled with a porous material. The numerical method includes finite volume discretization with the upwind scheme on structure orthogonal regular meshes. Linearization of the source term, which consists of viscous and form drags, increases the stiffness of the algebraic equation set. Performance of the correction storage (CS) multigrid algorithm is compared for different numbers of sweeps in each grid level. Up to four grids, for both multigrid V- and W- cycles, are considered. Effects of medium permeability and porosity on converged rates are presented. Results indicate that V-cycles perform slightly better in reducing the required computational effort and that the higher the permeability and the lower the porosity, faster solutions are obtained.

1. Introduction

Due to the growing applicability of porous media in many fields of engineering and science, such as petroleum extraction and processing, heat exchangers, filtration, combustion in porous matrices, electronic devices' cooling, to mention only a few, a good understanding of transport processes in such media is desirable.

Recently, turbulent flow [Pedras & de Lemos (2000, 2001a-c, 2003), Silva & de Lemos (2003a), de Lemos (2005)], heat [Rocamora & de Lemos (2000), Braga & de Lemos (2004), de Lemos & Braga (2003)] and mass transfer [de Lemos & Mesquita (2003), de Lemos & Tofaneli (2004)] in porous media has received much attention in the recent literature so that a growing demand for efficient computational schemes for flows through permeable structures is under way. In addition, laminar flow [Silva & de Lemos (2003b)] and heat transfer [Saito & de Lemos (2005)] in such media have also been considered. As such, a systematic evaluation of the efficiency of single-grid coupled numerical schemes [de Lemos (2000, 2003a-b)] and multigrid segregated solutions [Rabi & de Lemos (2001, 2003), Mesquita & de Lemos (2004)] have been obtained with aim of providing recommendations concerning the performance of such convergence acceleration methods.

These two numerical artifices for solution speed-up, namely block-solvers and multigrid methods, have been used simultaneously in Vanka (1986). The research effort here is being conducted with the purpose of evaluating them in separate. More specifically, in this work the multigrid method is under focus.

In regard to the use of multigrid schemes, the focus of the present work, its advantages are based on the following arguments. In most iterative numerical solutions, convergence rates of single-grid calculations are greatest in the beginning of the process, slowing down as the iterative process goes on. Effects like those get more pronounced as the grid becomes finer. Large grid sizes, however, are often needed when resolving small recirculating regions or detecting high heat transfer spots. The reason for this hard-to-converge behavior is that iterative methods can efficiently smooth out only those Fourier error components of wavelengths smaller than or comparable to the grid size. In contrast, Multigrid methods aim to cover a broader range of wavelengths through relaxation on more than one grid. The number of iterations and convergence criterion in each step along consecutive grid levels visited by the algorithm determines the cycling strategy, usually a V- or W-cycle. Within each cycle, the intermediate solution is relaxed before (pre-) and after (post-smoothing) the transportation of values to coarser (restriction) or to finer (prolongation) grids [Brandt (1977), Stüben & Trottenberg (1982), Hackbusch (1985), Sathiyamurthy & Patankar (1994), Thompson & Ferziger (1989)].

Accordingly, Multigrid methods can be roughly classified into two major categories. In the CS formulation algebraic equations are solved for the corrections of the variables whereas, in the full approximation storage (FAS) scheme, the variables themselves are handled in all grid levels. It has been pointed out in the literature that the application of the CS formulation is recommended for the solution of linear problems being the FAS formulation more suitable to non-linear cases [Brandt (1977), Stüben & Trottenberg (1982), Hackbusch (1985)]. An exception to this rule seems to be the work of Jiang, et al (1991), who reported predictions for the Navier-Stokes equations successfully applying the Multigrid CS formulation. In the literature, however, not too many attempts in solving non-linear problems with Multigrid linear operators are found.

Acknowledging the advantages of using multiple grids, Rabi & de Lemos (1998a) presented numerical computations applying this technique to recirculating flows in several geometries of engineering interest. There, the correction storage (CS) formulation was applied to non-linear problems. Later, Rabi & de Lemos (1998b), analyzed the effect of Peclet number and the use of different solution cycles when solving the temperature field within flows with a given velocity distribution. In all those cases, the advantages in using more than one grid in iterative solution was confirmed, furthermore, de Lemos & Mesquita (1999), introduced the solution of the energy equation in their Multigrid algorithm. Temperature distribution was calculated solving the whole equation set together with the flow field as well as uncoupling the momentum and energy equations. A study on optimal relaxation parameters was there reported. More recently Mesquita & de Lemos (2000a-b) analyzed the influence of the increase of points of the mesh and optimal values of the parameters of the Multigrid cycle for different geometries. Additionally, Rabi & de Lemos (2001, 2003), presented a study on optimal convergence characteristics in solution of conductive-convective problems.

Justification for the present contribution lies on the fact that most works on multigrid methodology deals with unobstructed flows rather than flow through permeable matrices. There seems then to be a lack in the literature of published material covering how a

multigrid solution behaves as a function of porous media properties such as permeability and porosity. As such, the present contribution extends the early work on CS Multigrid methods for clear (unobstructed) domains to the solution of flow in porous media. More specifically, steady-state laminar flow in a tank totally filled with porous material is calculated with up to 4 grids. A schematic of such configurations is show in Figure 1.

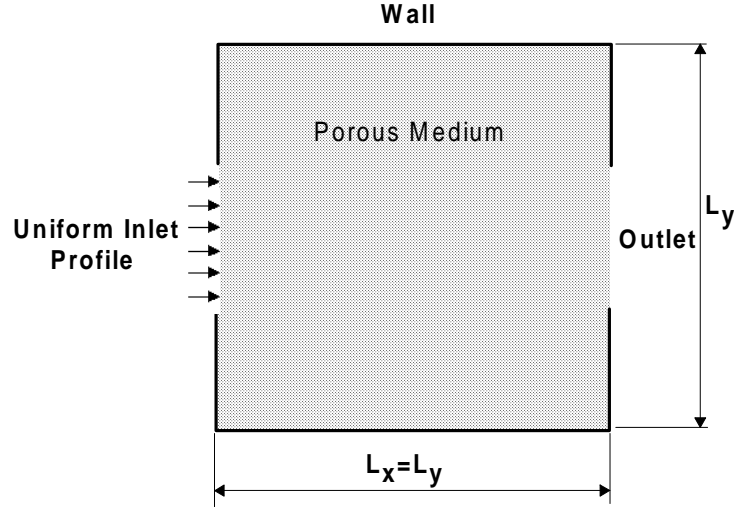


Figure 1: Geometry and boundary conditions

2. Governing Equations and Numerics

A macroscopic form of the governing equations is obtained by taking the volumetric average of the entire equation set. In this development, the porous medium is considered to be rigid, undeformable and saturated by an incompressible fluid.

The microscopic continuity equation for the fluid phase is given by:

$$\nabla \cdot \mathbf{u} = 0 \quad (1)$$

Applying the volume-average operator to equation (1), one has (see Pedras & de Lemos (2001) for details),

$$\nabla \cdot \mathbf{u}_D = 0 \quad (2)$$

The Dupuit-Forchheimer relationship, $\mathbf{u}_D = \phi \langle \mathbf{u} \rangle^i$, has been used where the operator “ $\langle \cdot \rangle$ ” identifies the intrinsic (liquid volume based) average of \mathbf{u}_D [Bear (1972), Gray & Lee (1977)]. Equation (2) represents the macroscopic continuity equation for an incompressible fluid in a rigid porous medium.

The microscopic Navier-Stokes equation for an incompressible fluid with constant properties can be written as,

$$\rho \nabla(\mathbf{u}\mathbf{u}) = -\nabla p + \mu \nabla^2 \mathbf{u} \quad (3)$$

Hsu & Cheng (1990) have applied the volume averaging procedure to equation (3) obtaining,

$$\nabla(\rho\phi\langle\mathbf{u}\mathbf{u}\rangle^i) = -\nabla(\phi\langle p\rangle^i) + \mu\nabla^2(\phi\cdot\langle\mathbf{u}\rangle^i) + \mathbf{R} \quad (4)$$

where

$$\mathbf{R} = \frac{\mu}{\Delta V} \int_{A_i} n(\nabla \cdot \mathbf{u}) dS - \frac{1}{\Delta V} \int_{A_i} np dS \quad (5)$$

The term \mathbf{R} represents the total drag per unit volume acting on the fluid by the action of the porous structure. A common model for it is known as the Darcy-Forchheimer extended model and is given by:

$$\mathbf{R} = - \left[\frac{\mu\phi}{K} \mathbf{u}_D + \frac{c_F \phi \rho |\mathbf{u}_D| \mathbf{u}_D}{\sqrt{K}} \right] \quad (6)$$

where the constant c_F is known in the literature as the non-linear Forchheimer coefficient, taken as 0.55 in all simulations for flow in porous media shown below. Is also important to clarify that c_F is a model constant and that it was not the objective of this work to investigate its influence on multigrid performance.

Then, making use of the expression $\mathbf{u}_D = \phi \langle \mathbf{u} \rangle^i$, equation (4) can be rewritten as,

$$\left[\nabla \left(\frac{\mathbf{u}_D \mathbf{u}_D}{\phi} \right) \right] = -\nabla(\phi\langle p\rangle^i) + \mu\nabla^2 \mathbf{u}_D - \left[\frac{\mu\phi}{K} \mathbf{u}_D + \frac{c_F \phi \rho |\mathbf{u}_D| \mathbf{u}_D}{\sqrt{K}} \right] \quad (7)$$

3. Numerical Model

The solution domain is divide into a number of rectangular control volumes (CV), resulting in a structure orthogonal non-uniform mesh. Grid points are locate according to a cell-centered scheme and velocities are store in a collocated arrangement (see Patankar & Spalding (1972) and Patankar (1980) for details on the CV method). A typical CV with its main dimensions and internodal distances is sketched in Figure 2

Writing equations (2) and (7) in terms of a general variable φ

$$\frac{\partial}{\partial x} \left(\rho U \varphi - \Gamma_\varphi \frac{\partial \varphi}{\partial x} \right) + \frac{\partial}{\partial y} \left(\rho V \varphi - \Gamma_\varphi \frac{\partial \varphi}{\partial y} \right) = S_\varphi \quad (8)$$

where φ stands for U and V (see details in Rabi & de Lemos (2001, 2003)). Integrating the equation (8) over the control volume of Figure 2,

$$\int_{\delta_v} \left[\frac{\partial}{\partial x} (\rho U \varphi) + \frac{\partial}{\partial y} (\rho V \varphi) \right] dv = \int_{\delta_v} \left[\frac{\partial}{\partial x} \left(\Gamma_\varphi \frac{\partial \varphi}{\partial x} \right) + \frac{\partial}{\partial y} \left(\Gamma_\varphi \frac{\partial \varphi}{\partial y} \right) \right] dv + \int_{\delta_v} S_\varphi dv \quad (9)$$

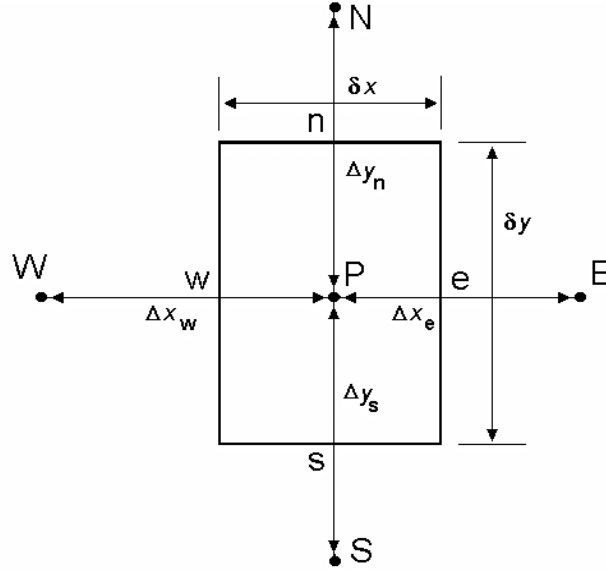


Figure 2: Control Volume for discretization

Integration of the three terms in (9), namely: convection, diffusion and source, lead to a set of algebraic equations. These practices are described elsewhere (e.g. Patankar (1980)) and for this reason they not repeated here. In summary, convective terms are discretized using the upwind differencing scheme (UDS), diffusive fluxes make use of the central differencing scheme.

Substitution of all approximate expressions for interface values and gradients into the integrated transport equation (9), gives the final discretization equation for grid node P

$$a_P \phi_P = a_E \phi_E + a_W \phi_W + a_N \phi_N + a_S \phi_S + b \quad (10)$$

with the east face coefficient, for example, being define as

$$a_E = \max[-C_e, 0] + D_e \quad (11)$$

In (11), $D_e = \mu_e \delta_y / \Delta x_e$ and $C_e = (\rho U)_e \delta_y$ are the diffusive and convective fluxes at the CV east face, respectively, and, as usual, the operator $\max[a, b]$ returns the greater between a and b.

4. Multigrid Technique

Assembling equation (10) for each control volume of Figure 2 in the domain of Figure 1 defines a linear algebraic equation system of the form,

$$A_k T_k = b_k \quad (12)$$

where A_k is the matrix of coefficients, T_k is the vector of unknowns and b_k is the vector accommodating source and extra terms. Subscript “ k ” refers to the grid level, with $k=1$ corresponding to the coarsest grid and $k=M$ to the finest mesh.

It is important to emphasize that the algebraic equation system (12) is *non-linear* in nature and that the most appropriated multigrid method for solving it, according to the literature, is the so called *full approximation storage* (FAS) formulation. However, the *correction storage* (CS) method can also be used to relax all variables if appropriate linearization of the entire equation set is applied (see Jiang, et al (1991), Rabi & de Lemos (2001, 2003), Mesquita & de Lemos (2004) for details).

As mentioned, Multigrid is here implemented in a correction storage formulation (CS) in which one seeks coarse grid approximations for the correction defined as $\delta_k = \mathbf{T}_k - \mathbf{T}_k^*$ where \mathbf{T}_k^* is an intermediate value resulting from a small number of iterations applied to (12). For a linear problem, one shows that δ_k is the solution of [Brandt (1977), Stüben & Trottenberg (1982), Hackbusch (1985)],

$$A_k \delta_k = r_k \quad (13)$$

where the residue is defined as

$$r_k = b_k - A_k T_k^* \quad (14)$$

Eq. (10) can be approximated by means of a coarse-grid equation,

$$A_{k-1} \cdot \delta_{k-1} = r_{k-1} \quad (15)$$

with the restriction operator I_k^{k-1} used to obtain

$$r_{k-1} = I_k^{k-1} r_k \quad (16)$$

The residue restriction is accomplished by summing up the residues corresponding to the four fine grid control volumes that compose the coarse grid cell. Thus, equation (16) can be rewritten as,

$$r_{k-1}^{IJ} = r_k^{IJ} + r_k^{ij+1} + r_k^{i+1j} + r_k^{i+1j+1} \quad (17)$$

Diffusive and convection coefficients in matrix A_k need also to be evaluated when changing grid level. Diffusive terms are recalculated since they depend upon neighbor grid node distances whereas coarse grid mass fluxes (convective terms) are simply added up at control volume faces. This operation is commonly found in the literature (Peric et al. (1989a), Peric, et al (1989b), Hortmann et al (1990)).

Once the coarse grid approximation for the correction δ_{k-1} has been calculated, the prolongation operator I_{k-1}^k takes it back to the fine grid as

$$\delta_k = I_{k-1}^k \delta_{k-1} \quad (18)$$

In order to update the intermediate value

$$T_k = T_k^* + \delta_k \quad (19)$$

Figure 3 illustrates a 4-grid iteration scheme for both the *V*- and *W*-cycles where the different operations are: *s*=smoothing, *r*=restriction, *cg*=coarsest grid iteration and *p*=prolongation. Also, the number of domain sweeps before and after grid change is denoted by v^{pre} and v^{post} , respectively. In addition, at the coarsest *k* level ($k=1$), the grid is swept v^{cg} times by the error smoothing operator.

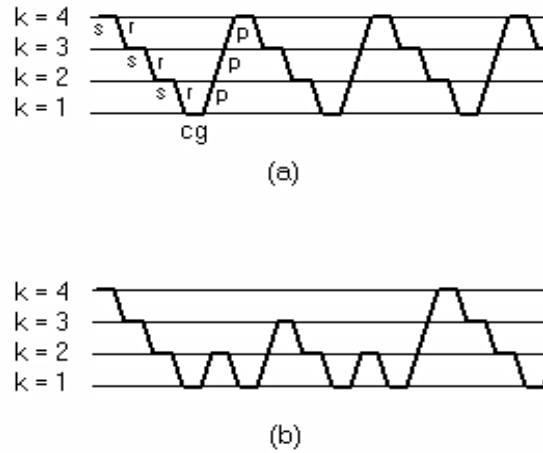


Figure 3: Sequence of operations in a 4-grid iteration scheme: a) V-cycle, b) W-cycle.

4. Results and Discussion

The computer code developed was run on a IBM PC machine with a processor AMD Athlon 1.3GHz. Grid independence studies were conducted such that the solutions presented herein are essentially grid independent. For both cycles, *pre*- and *post*-smoothing iterations were accomplished via the Gauss-Seidel algorithm while, at the coarsest-grid, the TDMA method has been applied (Patankar (1980)). Also, the geometry of Figure 1 was run with the finest grid having sizes of 66x66 grid points.

At a certain grid level, error smoothing operations were applied to all variables before the grid was changed. Relaxation parameters equal to 0.8, 0.8 e 0.6 were applied to the U , V and P equations, respectively. The sweeping strategy through all variables in the V- and W-cycles considered $v^{pre} = v^{post} = 2$ sweeps for both *pre*-, and *post*-smoothing iterations. At the coarsest grid, three iterations were applied, or say, $v^{cg} = 3$. Studies identifying optimal numbers for the *pre*- and *post*-sweeps can be found in Rabi & de Lemos (2001) and, Mesquita & de Lemos (2004).

With the aim of checking the accuracy of the numerical solution, after implementation of porous media model, the limiting case of flow in clear fluid was simulated by setting $\phi = 0.998$, $K = 1 \times 10^{10} \text{ m}^2$ and $c_F = 0$. Figure 4 shows velocity profiles at the exit of the tank. The figure indicates that the solution with the porous model reproduces the clear flow situation when appropriate parameters are used.

The residue of equation (9) is normalized and calculated according to

$$R_U = \sqrt{\sum_{ij} (R_{ij})^2} \quad (20)$$

with $R_{ij} = a_p U_p - (\sum_{nb} a_{nb} U_{nb})$ where subscript ij identifies a given control volume on the finest grid and nb refers to its neighboring control volumes.

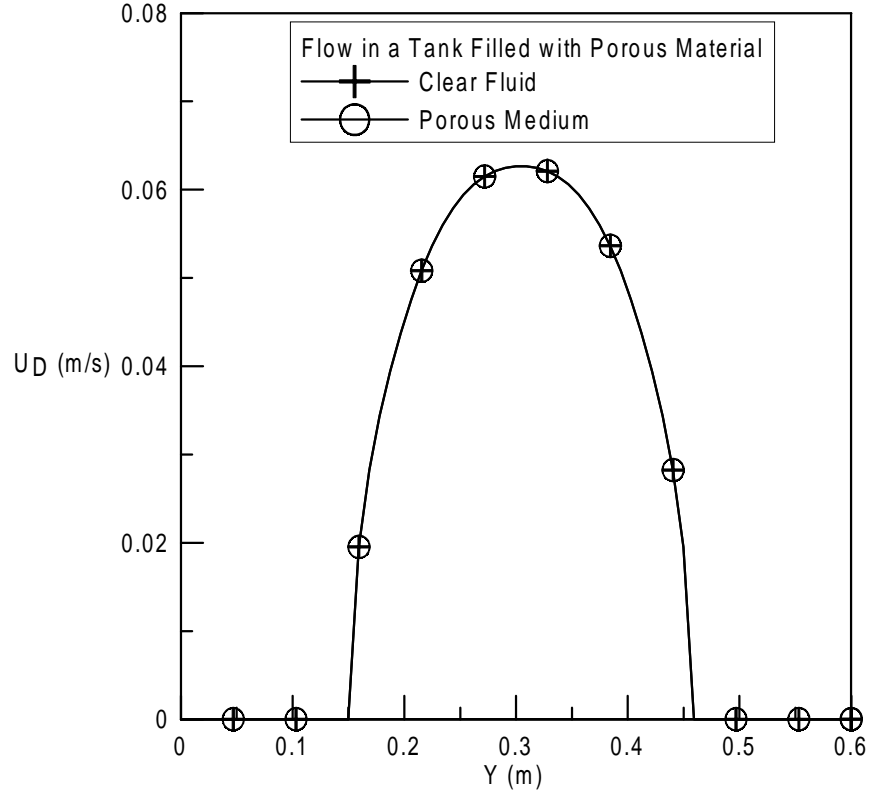


Figure 4: Velocity profiles at the exit of a tank for porous medium with $c_F=0.0$, $\phi=0.998$ and $K=1 \times 10^{10} \text{ m}^2$

Figure 5, shows the residue history for velocity component U, for $Re_{in} = 300$, up to 4 grids, for the V- and W-cycles. Reduction of the necessary computational time for solving the governing equations for flow in porous media is seen in the figures. For four grids, a slight advantage in using the V-cycle is observed in Fig. 5. For recirculating flows, the better performance of W-cycles over other sweeping strategies is documented in the literature [Jiang, et al (1991), Rabi & de Lemos (2001, 2003), Mesquita & de Lemos (2004)]. There, spending more time per cycle in coarser grids (see Figure 3) helps in smoothing out low frequency errors, which could be associated with the numerical resolution of recirculatory fluid motion. However, for flow in porous media and for the conditions here analyzed, cycling in between the grids with equal time spending per grid (V-cycle) seems to be slightly more economical, supposedly due to the fact that strong recirculating motion is usually absent due to the damping action of the porous matrix.

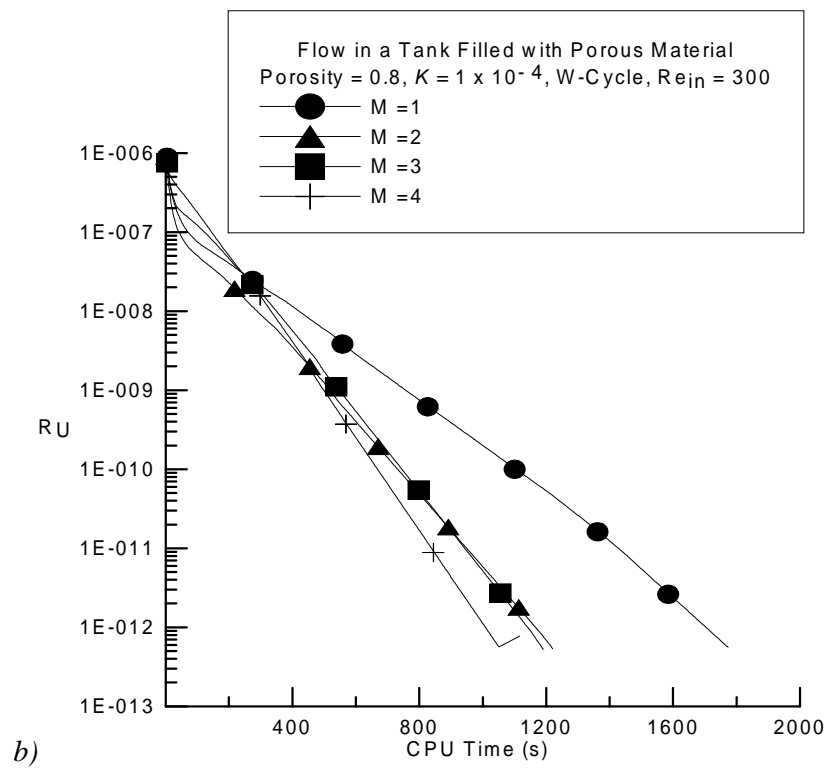
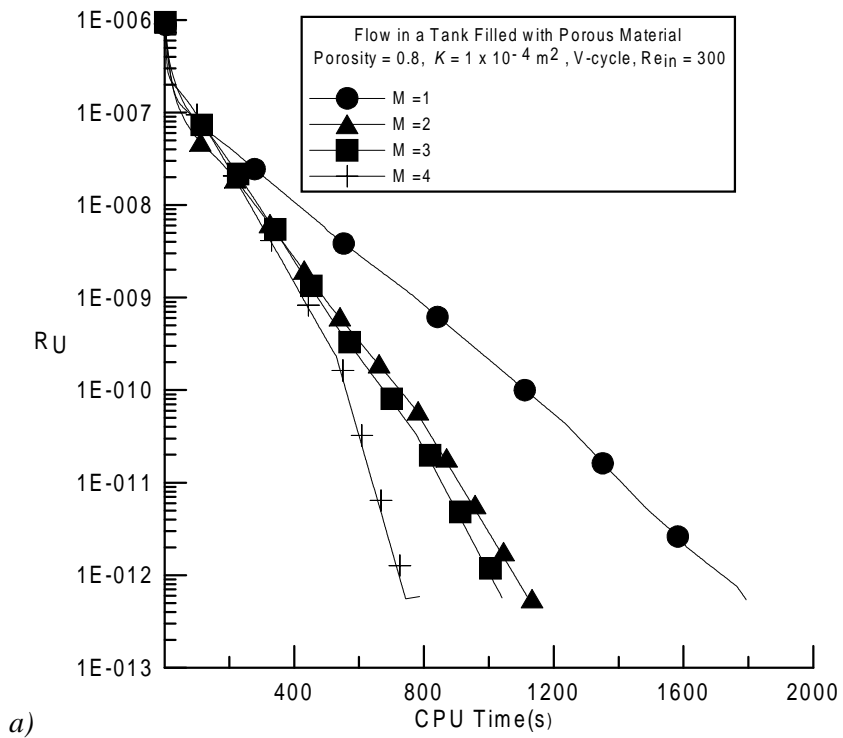


Figure 5: Residue history of U velocity component, $Re_{in} = 300$: a) V-cycle; b) W-cycle.

Figures 6, 7, and 8 and show the effect of permeability K on convergence rates for $Re_{in} = 300$, 600 and 900, respectively. The lower the permeability, more slowly the solution converges. A possible explanation for this behavior is based on numerical reasons, as follows.

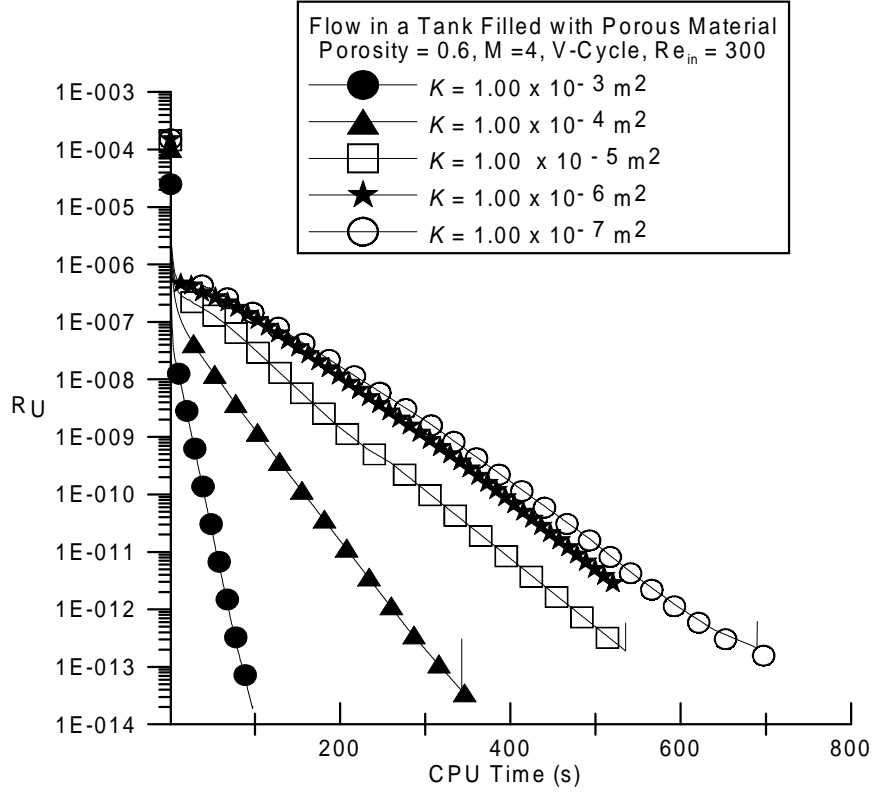


Figure 6: Effect of permeability K on residue history for 4-grids, $Re_{in} = 300$, $\phi = 0.6$

Inspecting equation (7) one can note that the two drag terms are dependent on the Darcy velocity \mathbf{u}_D and, as such, one could take advantage, during the discretization process, of a *linearization* of the source term (see Patankar (1980)). One can also note that as the value of K decreases, the relative importance of the two drag terms in equation 7 becomes greater. The Darcy-Forchheimer extended model in equation (5) is a representation of the viscous and form drags of equation (6), which are associated with the additional forces exerted by the porous matrix on the fluid phase (see Pedras & de Lemos (2001) for details). In the discretization process here followed, which originated equation (10), linearization of the source term was accomplished in the form

$$S_U = \overset{=0}{S_c} + S_p U = - \underbrace{\left[\frac{\mu \phi}{K} + \frac{c_F \phi \rho |\mathbf{u}_D|}{\sqrt{K}} \right]}_{s_p} U \quad (21)$$

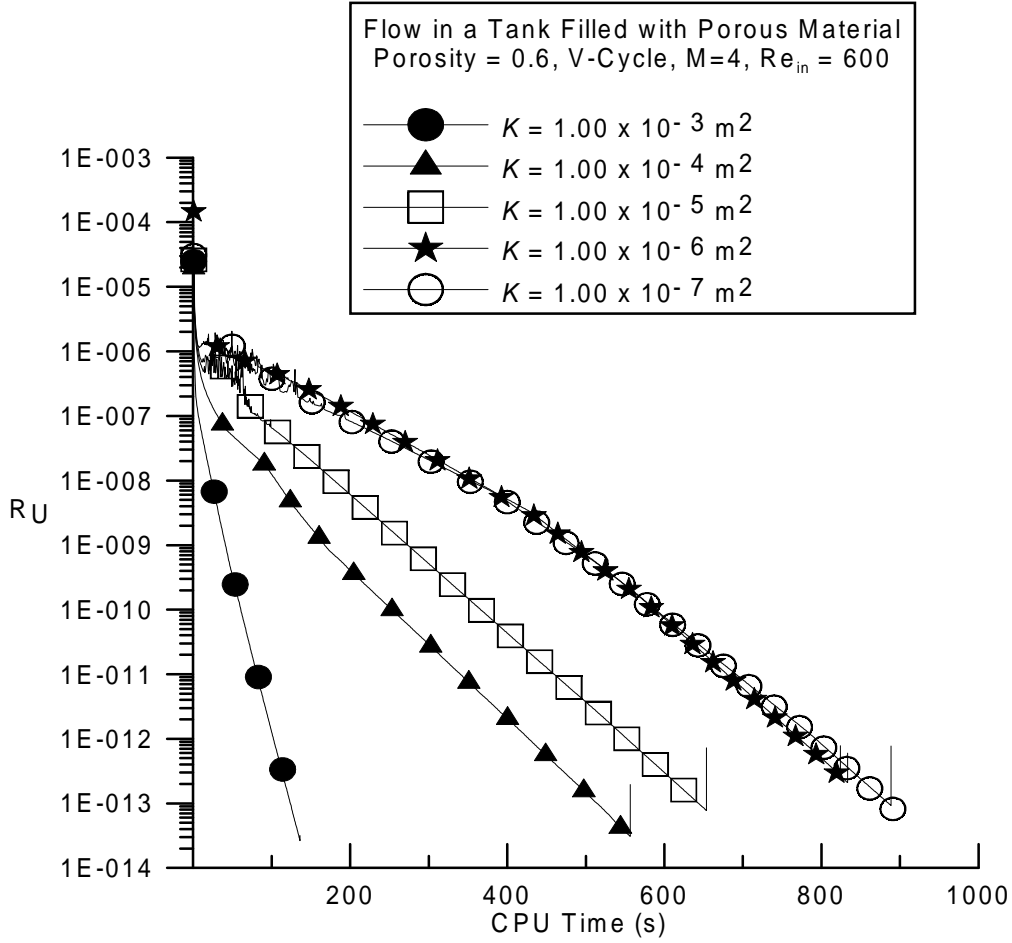


Figure 7: Effect of permeability K on residue history for 4-grids, $Re_{in} = 600$, $\phi = 0.6$

giving rise to the main coefficient,

$$a_p = \sum_{nb} a_{nb} - S_p \quad (22)$$

For each grid level k , coefficient a_p composes the main diagonal of A_k on the right of equation (12). Excessively lower values of K cause larger values of a_p leading to a matrix A_k with main diagonal dominance. The “stiffness” of the algebraic system is then largely increased leading eventually to difficulties in achieving convergence. In this work, equation (21) was applied and inclusion of \mathbf{R} (equation (5)) in the main coefficient a_p reduced the convergence rates for lower K values, as observed in Figures 6 to 8.

The effect of the medium porosity ϕ on the residue reduction rate, for $Re_{in} = 300$, is presented in Figure 9 for multigrid methodologies. For larger values of the porosity the stiffness of the algebraic system is also enhanced, as can be observed in equation (21). An increase in ϕ will yield a larger negative value for S_p , also increasing the main diagonal of A_k and, ultimately, implying in slower convergence rates.

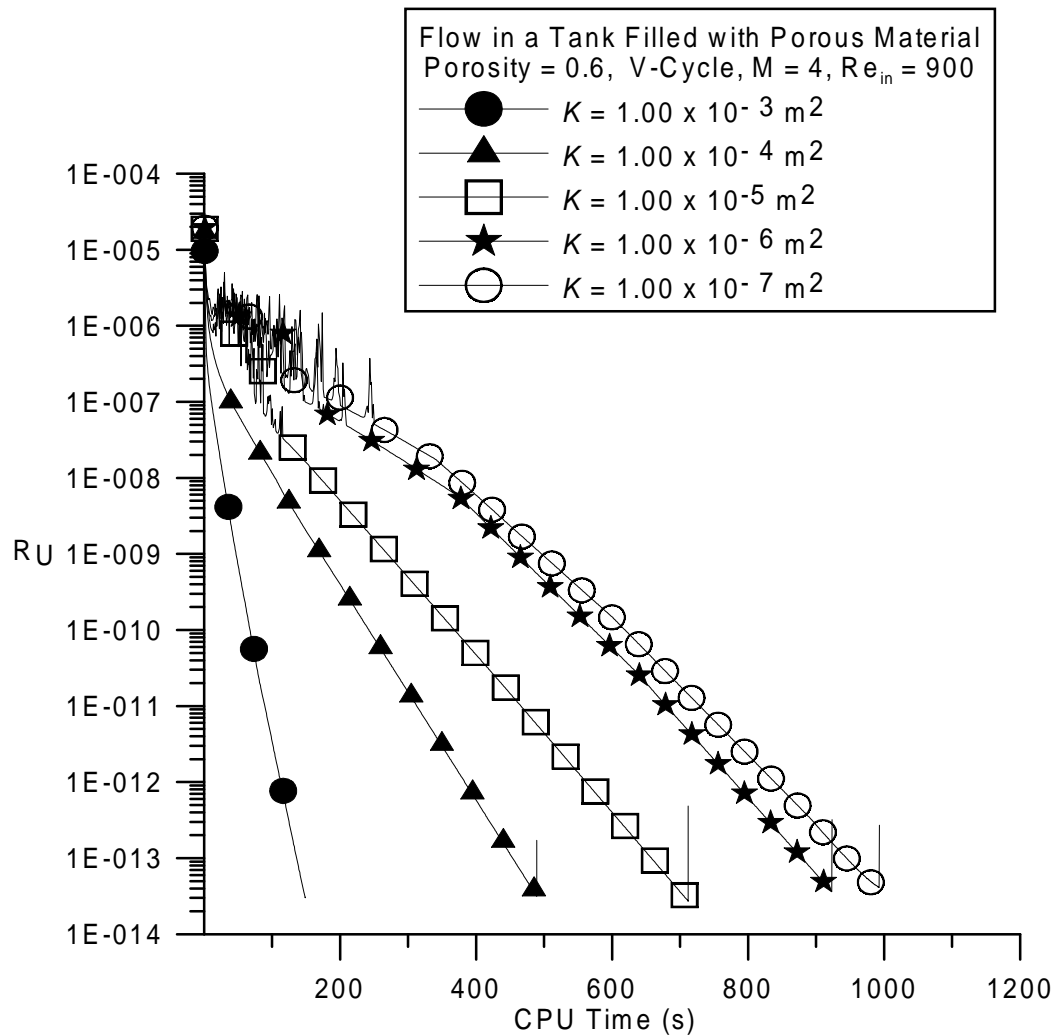


Figure 8: Effect of permeability K on residue history for 4-grids, $Re_{in} = 900$, $\phi = 0.6$

5. Conclusions

This work has numerically solved the flow governing equation for the geometry of a tank completely filled with a porous material. The multigrid technique has been used for increasing convergence rates. Linearization of the source term composed by the Darcy-Forchheimer extended model promoted the stability of the algebraic equation system. The results have shown that also for the porous medium model the use of more than one numerical grid is beneficial for reducing the computing time. Also, an increase in the permeability of the medium makes the system of equations less stiff and closer to the modeling of clear flow. Increasing the porosity of the medium, while keeping all other variables fixed, also reflected the enhancement of the numerical stability of the equation set. As a consequence, numerical solutions required more computational time.

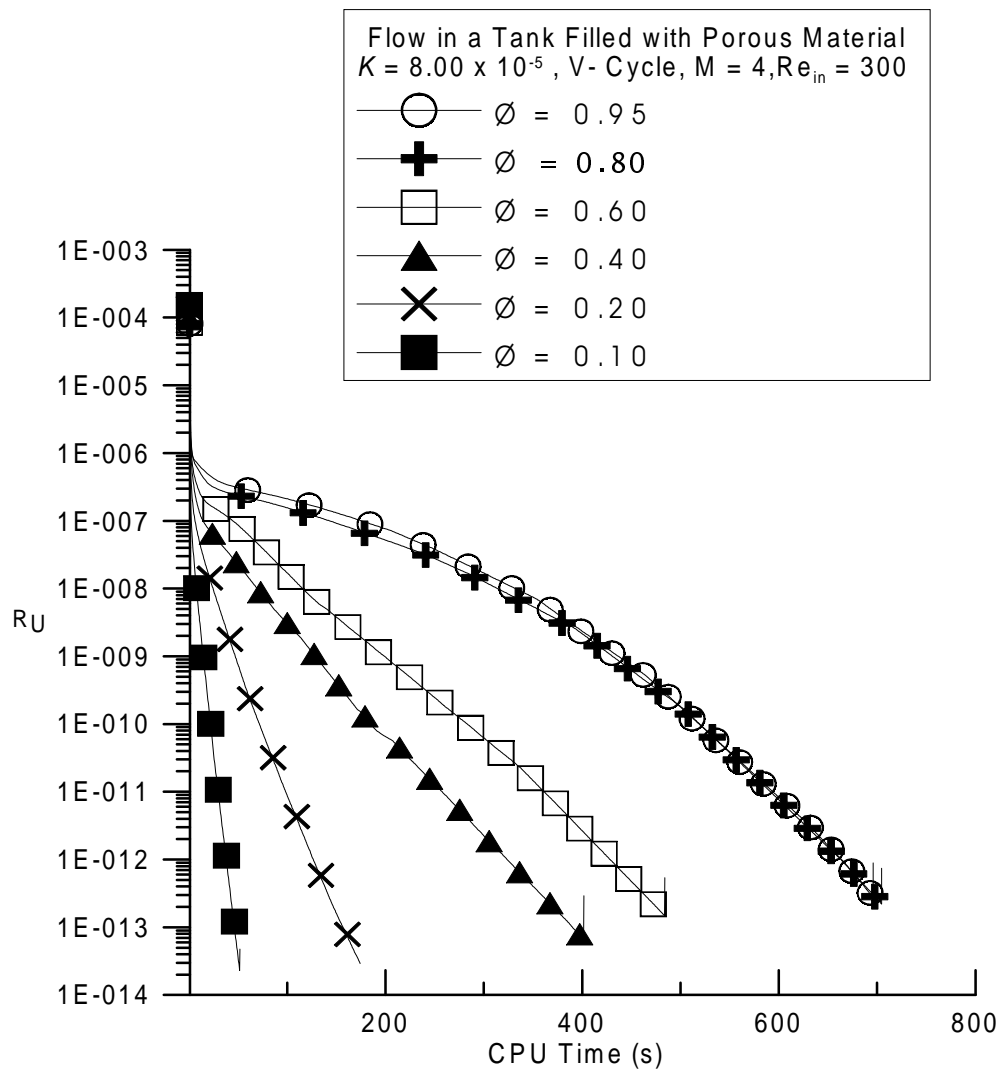


Figure 9: Effect porosity ϕ on residue history for 4 grids, $Re_{in} = 300$, $K = 8.00 \times 10^{-5} \text{ m}^2$.

Acknowledgments

The authors would like to thank CNPq and FAPESP, Brazil, for their financial help during the preparation of this work.

Nomenclature

c_F Forchheimer coefficient in eqn. (7)

CPU CPU Time (s)

K Permeability

L_x Domain length

L_y	Domain height
M	Maximum grid number
p	Thermodynamic pressure
Pe	Peclet Number
Pr	Prandtl Number
\mathbf{R}	Total drag per unit volume
Re	Reynolds Number
R_{ij}	Residue
S_φ	Source term for φ , $\varphi = U, V, p$
\mathbf{u}	Microscopic (local) velocity vector
\mathbf{u}_D	Darcy velocity vector (volume average over \mathbf{u}), $\mathbf{u}_D = \phi \langle \mathbf{u} \rangle^i$
$\langle \mathbf{u} \rangle^i$	Intrinsic (fluid) average of \mathbf{u}
$\langle p \rangle^i$	Intrinsic (fluid) average of pressure p
U	Component of velocity along x
V	Component of velocity along y
x, y	Cartesian coordinates

Subscript

i, j	Nodal index
in	input values
k	Grid level
nb	Neighboring

Greeks

μ	Dynamic viscosity
ρ	Density
ϕ	Porosity
φ	General variable
Γ_φ	Diffusion coefficient for φ , $\varphi = U, V, P$
ν^{cg}	Number of Coarsest-grid iterations
ν^{pre}	Number of pre-smoothing iterations
ν^{post}	Number of post-smoothing iterations

References

- [1] Bear, J., 1972, Dynamics of Fluids in Porous Media, Dover Publications
- [2] Braga, E.J., de Lemos, M.J.S., Turbulent Natural Convection in a Porous Square Cavity Computed with a Macroscopic k- ϵ Model, *Int. J. Heat Mass Transfer*, **47**(26), (2004) pp. 5639-5650.
- [3] Brandt, A., 1977 Multi-Level Adaptive Solutions To Boundary-Value Problems, *Math. Comp.*, **31**(138), pp. 333-390.
- [4] de Lemos, M.J.S., 2000, Flow And Heat Transfer In Rectangular Enclosures Using A New Block Implicit Numerical Method, *Numerical Heat Transfer - Part B*, **37**(4) pp. 489-508.
- [5] de Lemos, M.J.S., 2003a, A Block-Implicit Method for Numerical Simulation of Swirling Flows in a Model Combustor, *Int. Comm. Heat Mass Transfer*, **30**(3), pp. 369-378.
- [6] de Lemos, M.J.S., 2003b, A Block-Implicit Numerical Procedure For Simulation of Buoyant Swirling Flows in a Model Furnace, *International Journal for Numerical Methods in Fluids*, **43**(3), pp. 281 - 299.
- [7] de Lemos, M.J.S., 2005, Turbulent Kinetic Energy Distribution across the Interface between a Porous Medium and a Clear Region, *Int. Comm. Heat Mass Transfer*, **32**(1-2), pp. 107-115.
- [8] de Lemos, M.J.S., Braga, E.J., 2003, Modeling of Turbulent Natural Convection in Saturated Rigid Porous Media, *Int. Comm. Heat Mass Transfer*, **30**, (5), pp. 615-624.
- [9] de Lemos, M.J.S., Mesquita, M.S., 1999, Multigrid Numerical Solutions Of Non-Isothermal Laminar Recirculating Flows, *Applications of Computational Heat Transfer*, ASME-HTD-Vol. 364-3, ISSN: 0272-5673, ISBN: 0-7918-1656-7, Ed.L.C. White, Pg. 323-330.
- [10] de Lemos, M.J.S., Mesquita, M.S., 2003, Turbulent Mass Transport in Saturated Rigid Porous Media, *Int. Comm. Heat Mass Transfer*, **30**(1), pp. 105-113.
- [11] de Lemos, M.J.S., Tofaneli, L.A. 2004, Modeling of Double-Diffusive Turbulent Natural Convection in Porous Media, *Int. J. Heat Mass Transfer*, **47**(19-20), pp. 4221-4231.
- [12] Gray, W.G., Lee, P.C.Y., 1977 On the Theorems for Local Volume Averaging of Multiphase System, *Int. J. Multiphase Flow*, **3**, pp. 333-340.
- [13] Hackbusch, W., 1985, Multigrid Methods And Applications, Springer-Verlag, Berlin.
- [14] Hortmann, M., Peric, M., Scheuerer, G., 1990, Finite Volume Multigrid Prediction Of Laminar Convection: Bench-Mark Solutions, *Int. J. Num. Meth. Fluids*, **11**, pp. 189-207.
- [15] Hsu, C.T., Cheng, P., 1990, Thermal dispersion in a porous medium, *Int. J. Heat Mass Transfer*, **33**, pp. 1587-1597.
- [16] Hutchinson, B.R., Galpin, P.F., Raithby, G.D., 1988, Application of Additive Correction Multigrid To The Coupled Fluid Flow Equations, *Num. Heat Transfer*, **13**, pp. 133-147.
- [17] Jiang, Y., Chen, C.P., Tucker, P.K., 1991, Multigrid Solutions of Unsteady Navier-Stokes Equations Using a Pressure Method, *Num. Heat Transfer - Part A*, **20**, pp. 81-93.

- [18] Mesquita, M.S., de Lemos, M.J.S., 2000a, Numerical Solution of Non-Isothermal Laminar Recirculating Flows Using The Multigrid Method, ENCIT 2000, Porto Alegre, RS, Brazil, 2000.
- [19] Mesquita, M.S., de Lemos, M.J.S., 2000b, Multigrid Numerical Solutions of Laminar Back Step Flow, *Congresso Nacional de Engenharia Mecânica*, Natal, RN, Brazil.
- [20] Mesquita, M.S., de Lemos, M.J.S., 2004, Optimal Multigrid Solutions Of Two Dimensional Convection-Conduction Problems, *Applied Mathematics and Computation*, **152**(3), pp.725-742.
- [21] Patankar, S.V., 1980, Numerical Heat Transfer And Fluid Flow, Mc-Graw Hill.
- [22] Patankar, S.V., Spalding, D.B., 1972, A Calculation Procedure for Heat, Mass and Momentum Transfer in Three Dimensional Parabolic Flows, *Int. J. Heat Mass Transfer*, **15**, pp. 1787-1806.
- [23] Pedras, M.H.J., de Lemos, M.J.S., 2000, On the Definition of Turbulent Kinetic Energy for Flow in Porous Media, *Int. Comm. Heat Mass Transfer*, **27**(2), pp. 211-220.
- [24] Pedras, M.H.J., de Lemos, M.J.S., 2001a, Macroscopic Turbulence Modeling For Incompressible Flow Through Undeformable Porous Media, *Int. J. Heat Mass Transfer*, **44**(6), pp. 1081-1093.
- [25] Pedras, M.H.J., de Lemos, M.J.S., 2001b, Simulation of Turbulent Flow in Porous Media Using a Spatially Periodic Array and a Low Re Two-Equation Closure, *Numer. Heat Transfer, Part A-Appl.*, **39**(1), pp. 35-59.
- [26] Pedras, M.H.J., de Lemos, M.J.S., 2001c, On Mathematical Description and Simulation of Turbulent Flow in a Porous Medium Formed by an Array of Elliptic Rods, *ASME Journal of Fluids Engineering*, **123**(4), pp. 941-947.
- [27] Pedras, M.H.J., de Lemos, M.J.S., 2003, Computation of Turbulent Flow in Porous Media Using a Low Reynolds k- ϵ Model and an Infinite Array of Transversally Displaced Elliptic Rods, *Numer. Heat Transfer; Part A-Appl.*, **43**(6), pp. 585-602.
- [28] Peric M., R ger M., Scheurer G., 1989a, A Finite Volume Multigrid Method For Predicting Periodically Fully Developed Flow, *Int. J. Num. Fluids*, 18, pp.843-852.
- [29] Peric, M., R ger, M., Scheurer, G., 1989b, A Finite Volume Multigrid Method For Calculating Turbulent Flows, In: *Seventh Symposium On Turbulent Shear Flows*, pp. 7.3.1-7.3.6, Standford University.
- [30] Rabi, J.A., de Lemos, M.J.S., 1998a, Multigrid Numerical Solution of Incompressible Laminar Recirculating Flows, ENCIT98- *Proc. of 7th Braz. Cong. Eng. Th. Sci.*, vol. 2, pp. 915-920, Rio de Janeiro, RJ, Nov. 3-6.
- [31] Rabi, J.A., de Lemos, M.J.S., 1998b, The Effects Of Peclet Number And Cycling Strategy On Multigrid Numerical Solutions Of Convective-Conductive Problems, *7th AIAA/ASME Jnt Thermcs & HT Conf*, **Paper AIAA-98-2584**, Albuquerque, New Mexico, USA, June 15-18.
- [32] Rabi, J.A., de Lemos, M.J.S., 2001, Optimization of Convergence Acceleration in Multigrid Numerical Solutions of Conductive-Convective Problems, *Applied Mathematics and Computation*, **124**, pp. 215-226.

- [33] Rabi, J.A., de Lemos, M.J.S., 2003, Multigrid Correction-Storage Formulation Applied to the Numerical Solution of Incompressible Laminar Recirculating Flows, *Applied Mathematical Modelling*, **27**(9), pp. 717-732.
- [34] Rocamora, F. D. Jr., de Lemos, M.J.S., Analysis of Convective Heat Transfer for Turbulent Flow in Saturated Porous Media, *Int. Comm. Heat Mass Transfer*, **27**(6), pp. 825-834.
- [35] Raithby, G.D., Torrance, K.E., 1974, Upstream-Weighted Differencing Schemes And Their Application To Elliptic Problems Involving Fluid Flow, *Comp. & Fluids*, **2**, pp. 191-206.
- [36] Saito, M., de Lemos, M.J.S., Interfacial Heat Transfer Coefficient for Non-Equilibrium Convective Transport in Porous Media, *Int. Comm. Heat Mass Transfer*, **32**(5), (2005) pp. 667-677.
- [37] Sathyamurthy, P.S., Patankar, S.V., 1994, Block-Correction-Based Multigrid Method For Fluid Flow Problems, *Numerical Heat Transfer - Part B*, **25**, pp. 375-394.
- [38] Silva, R.A., de Lemos, M.J.S., 2003a, Turbulent flow in a channel occupied by a porous layer considering the stress jump at the interface, *Int. J. Heat Mass Transfer*, **46**(26), pp. 5113-5121
- [39] Silva, R.A., de Lemos, M.J.S., 2003b, "Numerical Analysis of The Stress Jump Interface Condition For Laminar Flow Over a Porous Layer", *Numerical Heat Transfer: Part A: Applications*, **43**(6), pp. 603-617.
- [40] Stüben, K., Trottenberg, U., 1982, Multigrid Methods, In *Lect. Notes Math.*, **960**, pp. 1-76, Berlin
- [41] Thompson, M.C., Ferziger, J.H., 1989, An Adaptive Multigrid Technique For The Incompressible Navier-Stokes Equations, *J. Comp. Phys.*, **82**, pp. 94-121.
- [42] Vanka, S.P. 1986, Block-Implicit Multigrid Calculation Of Two-Dimensional Recirculating Flows, *Comp. Meth. Appl. Mech. Eng.*, **86**, pp. 29-48.